Available online at www.sciencedirect.com
ScienceDirect
Automatica 43 (2007) 1832–1839
automatica
www.elsevier.com/locate/automatica

Brief paper

Extremum seeking for moderately unstable systems and for autonomous vehicle target tracking without position measurements☆

Chunlei Zhang[a], Antranik Siranosian[b], Miroslav Krstić[b,*]

[a]Etch Engineering Technology, Applied Materials, Santa Clara, CA, USA
[b]Department of Mechanical and Aerospace Engineering, University of California, San Diego, La Jolla, CA 92093-0411, USA

Received 30 September 2005; received in revised form 17 April 2006; accepted 12 March 2007
Available online 3 August 2007

Abstract

We remove the long standing restriction that plant dynamics in extremum seeking control must be stable and provide an extension that allows single integrators, double integrators, and moderately unstable single poles. An application of the result for single and double integrators is in control of autonomous vehicles. Extremum seeking is used for finding a source of a signal (chemical, electromagnetic, etc.) whose strength decays with the distance. This is achieved without the measurement of the position vector and using only the measurement of the scalar signal.

Keywords: Extremum seeking for moderately unstable systems; Averaging; Autonomous vehicles; Adaptive control

1. Introduction

Recent advances in extremum seeking have been followed by several exciting applications in non-model based control and optimization (Banaszuk, Narayanan, & Zhang, 2003; Peterson & Stefanopoulou, 2004; Popovic, Jankovic, Manger, & Teel, 2003; Li, Rotea, Chiu, Mongeau, & Paek, 2005; Zhang, Dawson, Dixon, & Xian, 2004). However, extremum seeking has so far been developed only for plants that are open loop stable (Ariyur & Krstić, 2003), with poles that are sufficiently well damped. In this paper we introduce a new idea how to extend the applicability of extremum seeking to marginally stable systems and moderately unstable systems. While the later extension is of general interest, the former comes from an application.

Control of autonomous vehicles is an immensely active area. Typically autonomous agents are allowed information sharing and are supplied with at least their position measurements. In this paper we use extremum seeking to address a problem with complete autonomy—a vehicle, without any position or velocity information, tracks the source of a scalar valued "concentration"-type signal (for example, the concentration of a chemical agent, or the strength of an acoustic, or an electromagnetic signal). The concentration field is not known, however, it is assumed to be the strongest at the source and to decay away from it. Therefore, the non-model based extremum seeking method is appropriate to approach this problem.

The classical extremum seeking scheme is modified for the stated task by observing that the integrator, a key adaptation element, is already present in vehicle models where the primary forces or moments acting on the vehicle are those that provide thrust/propulsion, i.e., for vehicles that act primarily in the $m\ddot{x} = F$ manner, where F is the motion-generating input and $\ddot{x}$ is the acceleration vector. In this paper we present results for a point mass model in the plane. An extension to 3D for a fully actuated vehicle is trivial, except that one employs separate probing frequencies in the ES algorithm for the individual axes of motion. The extension to point mass models with extensive losses (due for example to drag) is straightforward by noting that the input–output relationship drops in relative degree, making the problem actually easier. Drift-inducing forces like gravity or buoyancy are automatically accommodated by extremum seeking which auto-tunes the input to compensate for such constant disturbances.

☆ This paper was not presented at any IFAC meeting. This paper was recommended for publication in revised form by Associate Editor Andrew R. Teel under the direction of Editor Hassan Khalil.

* Corresponding author. Tel.: +1 858 822 1374; fax: +1 858 822 3107.
E-mail addresses: Chunlei_Zhang@amat.com (C. Zhang), asiranosian@ucsd.edu (A. Siranosian), krstic@ucsd.edu (M. Krstić).

0005-1098/$ - see front matter
doi:10.1016/j.automatica.2007.03.009

An extension to underactuated or non-holonomic vehicles is not straightforward and is the subject of Zhang, Arnold, Ghods, Siranosian, and Krstic (2007) another follow-up research.

The stability results we prove are local. The techniques introduced by Tan, Nesic, and Mareels (2005) can be used to achieve semi-global versions of our results.

2. A Velocity-actuated point mass (single integrators)

In the plane, an autonomous vehicle is modeled as a point mass:

$$\dot{x} = v_x, \quad \dot{y} = v_y, \tag{1}$$

where $[x, y]$ is the position of the point mass and v_x, v_y are the velocity inputs. Our method is extended later in the paper to the case where the inputs are forces; however, for clarity in introducing the new concept, we consider the simplest case of a velocity-actuated point mass first.

A block diagram of extremum seeking is shown in Fig. 1. The nonlinear map represents the distribution of the signal being tracked, whose strength will typically decay away from the origin, thus we assume that the nonlinear map $J = f(x, y)$ has a local maximum and pursue local tracking of that maximum. For clarity we assume that the nonlinear map is quadratic and that its Hessian is diagonal, viz.,

$$J = f(x, y) = f^* - q_x(x - x^*)^2 - q_y(y - y^*)^2, \tag{2}$$

where (x^*, y^*) is the *unknown* maximizer, $f^* = f(x^*, y^*)$ is the *unknown* maximum, and q_x, q_y are some *unknown* positive constants. General non-quadratic maps with non-diagonal Hessians are equally amenable to analysis, using the same technique as in Ariyur and Krstić (2003) and Krstić and Wang (2000). We show next that extremum seeking drives the autonomous vehicle to (x^*, y^*) without employing any knowledge of $f(x, y)$ or the measurements of (x, y), only the measurement of the output J of the nonlinear map $f(x, y)$. This corresponds to the problem of source localization in an unknown concentration field. The designer chooses the parameters $\alpha, \omega, h, c_x, c_y$ in the block diagram (Fig. 1), whereas the extremum seeking automatically tunes v_x, v_y to lead the vehicle to the peak of $f(x, y)$.

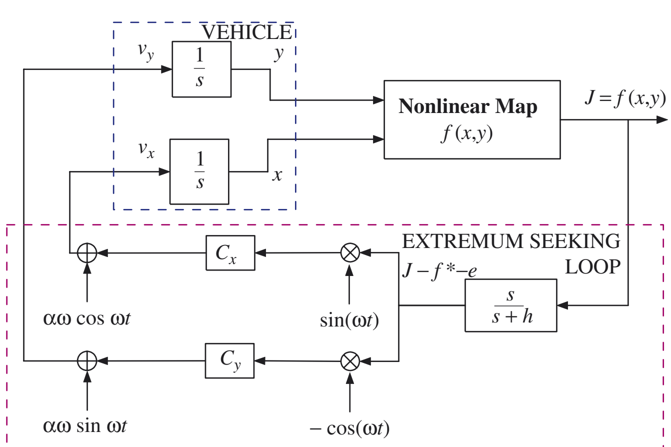

Fig. 1. Extremum seeking for velocity-actuated point mass.

The analysis that follows employs the averaging method. Let

$$e = \frac{h}{s+h}[J] - f^*, \tag{3}$$

then the signal after the washout filter can be expressed as $(s/(s+h))[J] = J - (h/(s+h))[J] = J - f^* - e$. Now, let us introduce the new coordinates

$$\tilde{x} = x - x^* - \alpha \sin(\omega t), \tag{4}$$

$$\tilde{y} = y - y^* + \alpha \cos(\omega t). \tag{5}$$

Then, in the time scale $\tau = \omega t$, we define:

$$\begin{aligned} \Delta &= (J - f^* - e) \\ &= -[q_x(\tilde{x} + \alpha \sin \tau)^2 + q_y(\tilde{y} - \alpha \cos \tau)^2 + e]. \end{aligned} \tag{6}$$

So we summarize the system in Fig. 1 as

$$\frac{\mathrm{d}\tilde{x}}{\mathrm{d}\tau} = +\frac{1}{\omega} c_x \Delta \sin \tau, \tag{7}$$

$$\frac{\mathrm{d}\tilde{y}}{\mathrm{d}\tau} = -\frac{1}{\omega} c_y \Delta \cos \tau, \tag{8}$$

$$\frac{\mathrm{d}e}{\mathrm{d}\tau} = +\frac{h}{\omega} \Delta. \tag{9}$$

System (7)–(9) is in the form to which the averaging method is applicable, provided $1/\omega$ is small, i.e., provided ω is large (relative to the other parameters in the extremum seeking scheme and relative to the parameters in the nonlinear map). The average model of (7)–(9) is

$$\frac{\mathrm{d}\tilde{x}_{\text{avg}}}{\mathrm{d}\tau} = -\frac{1}{\omega} \alpha c_x q_x \tilde{x}_{\text{avg}}, \tag{10}$$

$$\frac{\mathrm{d}\tilde{y}_{\text{avg}}}{\mathrm{d}\tau} = -\frac{1}{\omega} \alpha c_y q_y \tilde{y}_{\text{avg}}, \tag{11}$$

$$\frac{\mathrm{d}e_{\text{avg}}}{\mathrm{d}\tau} = -\frac{1}{\omega} h \left[q_x \tilde{x}^2_{\text{avg}} + q_y \tilde{y}^2_{\text{avg}} + e_{\text{avg}} + \frac{\alpha^2}{2}(q_x + q_y) \right]. \tag{12}$$

Then the equilibrium of the average model (10)–(12) is

$$\tilde{x}^e_{\text{avg}} = 0, \quad \tilde{y}^e_{\text{avg}} = 0, \quad e^e_{\text{avg}} = -\frac{\alpha^2}{2}(q_x + q_y). \tag{13}$$

The Jacobian of (10)–(12) at $(\tilde{x}^e_{\text{avg}}, \tilde{y}^e_{\text{avg}}, e^e_{\text{avg}})$ is

$$J_{\text{avg}} = \frac{1}{\omega} \begin{bmatrix} -\alpha c_x q_x & 0 & 0 \\ 0 & -\alpha c_y q_y & 0 \\ 0 & 0 & -h \end{bmatrix}. \tag{14}$$

Given the knowledge that the extremum is a maximum, it follows that q_x, q_y are known to be positive, though their actual values are unknown. Therefore, if we choose $\alpha > 0$, $c_x > 0$, $c_y > 0$ and $h > 0$, the Jacobian (14) is Hurwitz and the equilibrium (10)–(13) of the average system (12) is locally exponentially stable. Then according to the averaging theorem (Khalil, 2001), we have the following result.

Theorem 1. *There exists $\bar{\omega}$ such that for all $1/\omega \in (0, 1/\bar{\omega})$ the system in Fig. 1 with the nonlinear map of the form*

(2) *has a unique exponentially stable periodic solution* $(\tilde{x}^{2\pi/\omega}, \tilde{y}^{2\pi/\omega}, e^{2\pi/\omega})$ *of period* $2\pi/\omega$ *and this solution satisfies*

$$\left\| \begin{bmatrix} \tilde{x}^{2\pi/\omega} \\ \tilde{y}^{2\pi/\omega} \\ e^{2\pi/\omega} + \frac{\alpha^2}{2}(q_x + q_y) \end{bmatrix} \right\| \leqslant O(1/\omega), \quad \forall \tau \geqslant 0. \tag{15}$$

Since $x - x^* = \tilde{x} + \alpha \sin(\omega t) = (\tilde{x} - \tilde{x}^{2\pi/\omega}) + (\tilde{x}^{2\pi/\omega} - 0) + \alpha \sin\tau$, the theorem implies that the first term converges to zero, the second term is $O(1/\omega)$, and the third term is $O(\alpha)$. Thus $\limsup_{\tau\to\infty}|x - x^*| = O(\alpha + 1/\omega)$. Similarly, we can obtain $\limsup_{\tau\to\infty}|y - y^*| = O(\alpha + 1/\omega)$. Hence, we get

$$\limsup_{\tau\to\infty} |f - f^*| = O(\alpha^2 + (1/\omega)^2), \tag{16}$$

which characterizes the asymptotic performance of the extremum seeking loop in Fig. 1. Since we choose α as small and ω as large, the tracking error is very small.

Extremum seeking can be used for tracking of slowly varying trajectories, i.e., for tracking moving signal sources. When the trajectories are periodic our stability proof extends with very minor modifications which we do not present here in the interest of space. For example, consider a target motion is in the shape of the number eight (8):

$$x^* = a_m \sin(\omega_m t), \tag{17}$$

$$y^* = a_m \cos(2\omega_m t + \phi_m), \tag{18}$$

where $\omega_m \ll \omega$. If ω and ω_m are commensurate, i.e., if there exist natural numbers N and N_m such that $\omega/\omega_m = N/N_m$, then our proof extends, with averaging applied over a period of $2\pi N$ in the τ-time scale to account for the presence of an additional periodic terms on the right-hand sides of (7) and (8). If, however, ω and ω_m are incommensurate (for example, $\omega=4\pi\omega_m$ or $\omega=3\sqrt{23}\omega_m$), the technique of general averaging for "almost periodic" systems (Khalil, 2001, Section 10.6) leads to the same stability conclusions.

We first illustrate the simulation results of seeking a stationary target. The point mass model (1) and the quadratic map (2) are used in the simulation. We set the parameters of the target as $(x^*, y^*) = (-1, -1)$, $f^* = 1$, $q_x = 1$ and $q_y = 0.5$. The parameters of the extremum seeking loop are chosen as $\omega = 30$, $\alpha = 0.08$, $c_x = c_y = 10$ and $h = 1$. The starting position of the autonomous vehicle is $(x(0), y(0)) = (1, 1)$. As shown in Fig. 4(b), the autonomous vehicle starts at $(1, 1)$ by probing around to climb the gradient of the unknown map, eventually circling very closely around the maximizer $(-1, -1)$, the output of the unknown signal J is shown in Fig. 4(a), while the control inputs are shown in Fig. 4 (c) and (d). Note that the simulation results given in Fig. 4 are not for parameter values that are tuned to exhibit the best possible results. On the contrary, they illustrate the performance one would achieve for particularly poorly chosen parameter of the extremum seeking scheme. The point of showing the "worst case" performance is because the map being optimized is unknown, therefore it makes sense to ask a question about the performance with poorly chosen parameters.

For the slow time varying target (17)–(18), the simulation results are shown in Fig. 5, where we let $a_m = 1$, $\omega_m = 0.1$, $\phi_m = 3$, $f^* = 1$, $q_x = 1$, $q_y = 0.5$, and $\omega = 30$, $\alpha = 0.05$, $c_x = c_y = 15$, $h = 1$. The starting position of the autonomous vehicle is still $(x(0), y(0)) = (1, 1)$. The autonomous vehicle catches up with the target and then follows it quite closely in its number eight motion.

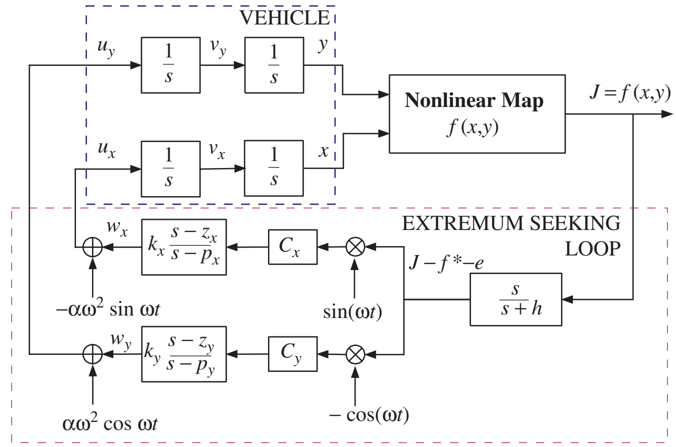

Fig. 2. Extremum seeking for force-actuated point mass.

3. A force-actuated point mass (double integrators)

In this section we present a modified scheme for force actuated point mass models, which instead of single integrators include double integrators. Both the vehicle model and the modified ES scheme are shown in Fig. 2. One can observe the double integrators in the vehicle model and the presence of phase lead compensators of the form $G(s) = k_c(s - z_0)/(s - p_0)$ whose role is to recover some of the phase in the feedback loop lost due to the addition of the second integrator. Four new states are introduced due to the PD compensators w_x, w_y and the additional integrators v_x, v_y. Again, we introduce the new coordinates $\tilde{v}_x = v_x - \alpha\omega\cos(\omega t)$, $\tilde{v}_y = v_y - \alpha\omega\sin(\omega t)$. Then, in the time scale $\tau = \omega t$, we summarize the system in Fig. 2 as

$$\frac{\mathrm{d}\tilde{x}}{\mathrm{d}\tau} = \frac{1}{\omega}\tilde{v}_x, \quad \frac{\mathrm{d}\tilde{y}}{\mathrm{d}\tau} = \frac{1}{\omega}\tilde{v}_y, \tag{19}$$

$$\frac{\mathrm{d}e}{\mathrm{d}\tau} = \frac{h}{\omega}\Delta, \tag{20}$$

$$\frac{\mathrm{d}\tilde{v}_x}{\mathrm{d}\tau} = \frac{1}{\omega}w_x, \quad \frac{\mathrm{d}\tilde{v}_y}{\mathrm{d}\tau} = \frac{1}{\omega}w_y, \tag{21}$$

$$\frac{\mathrm{d}w_x}{\mathrm{d}\tau} = \frac{1}{\omega}\left[p_x w_x - c_x k_x z_x \Delta \sin\tau + c_x k_x \omega \Delta \cos\tau + c_x k_x \frac{\mathrm{d}\Delta}{\mathrm{d}t}\sin\tau\right], \tag{22}$$

$$\frac{\mathrm{d}w_y}{\mathrm{d}\tau} = \frac{1}{\omega}\left[p_y w_y + c_y k_y z_y \Delta \cos\tau + c_y k_y \omega \Delta \sin\tau - c_y k_y \frac{\mathrm{d}\Delta}{\mathrm{d}t}\cos\tau\right], \tag{23}$$

where Δ is defined in (6), and $\mathrm{d}\Delta/\mathrm{d}t = -2q_x(\tilde{x} + \alpha\sin(\omega t))(\tilde{v}_x + \alpha\omega\cos(\omega t)) - 2q_y(\tilde{y} - \alpha\cos(\omega t))(\tilde{v}_y + \alpha\omega\sin(\omega t)) - h\Delta$.

The average model of (19)–(23) is

$$\frac{\mathrm{d}\tilde{x}_{\mathrm{avg}}}{\mathrm{d}\tau}=\frac{1}{\omega}\tilde{v}_{x\,\mathrm{avg}},\quad \frac{\mathrm{d}\tilde{y}_{\mathrm{avg}}}{\mathrm{d}\tau}=\frac{1}{\omega}\tilde{v}_{y\,\mathrm{avg}}, \tag{24}$$

$$\frac{\mathrm{d}e_{\mathrm{avg}}}{\mathrm{d}\tau}=\frac{1}{\omega}(-h)\left[q_x\tilde{x}_{\mathrm{avg}}^2+q_y\tilde{y}_{\mathrm{avg}}^2+e_{\mathrm{avg}}+\frac{\alpha^2}{2}(q_x+q_y)\right], \tag{25}$$

$$\frac{\mathrm{d}\tilde{v}_{x\,\mathrm{avg}}}{\mathrm{d}\tau}=\frac{1}{\omega}w_{x_{\mathrm{avg}}},\quad \frac{\mathrm{d}\tilde{v}_{y\,\mathrm{avg}}}{\mathrm{d}\tau}=\frac{1}{\omega}w_{y_{\mathrm{avg}}}, \tag{26}$$

$$\frac{\mathrm{d}w_{x_{\mathrm{avg}}}}{\mathrm{d}\tau}=\frac{1}{\omega}[p_x w_{x_{\mathrm{avg}}}+\alpha c_x k_x q_x(z_x+h)\tilde{x}_{\mathrm{avg}}-\alpha c_x k_x q_x\tilde{v}_{x\,\mathrm{avg}}], \tag{27}$$

$$\frac{\mathrm{d}w_{y_{\mathrm{avg}}}}{\mathrm{d}\tau}=\frac{1}{\omega}[p_y w_{y_{\mathrm{avg}}}+\alpha c_y k_y q_y(z_y+h)\tilde{y}_{\mathrm{avg}}-\alpha c_y k_y q_y\tilde{v}_{y\,\mathrm{avg}}], \tag{28}$$

and its equilibrium is

$$\tilde{x}_{\mathrm{avg}}^e=\tilde{y}_{\mathrm{avg}}^e=\tilde{v}_{x\,\mathrm{avg}}^{\,e}=\tilde{v}_{y\,\mathrm{avg}}^{\,e}=w_{x_{\mathrm{avg}}}^e=w_{y_{\mathrm{avg}}}^e=0, \tag{29}$$

$$e_{\mathrm{avg}}^e=-\frac{\alpha^2}{2}(q_x+q_y). \tag{30}$$

The Jacobian of (28) at the equilibrium $(\tilde{x}_{\mathrm{avg}}^e,\ \tilde{v}_{x\,\mathrm{avg}}^{\,e},\ w_{x_{\mathrm{avg}}}^e,\ \tilde{y}_{\mathrm{avg}}^e,\ \tilde{v}_{y\,\mathrm{avg}}^{\,e},\ w_{y_{\mathrm{avg}}}^e,\ e_{\mathrm{avg}}^e)$ is

$$J_{\mathrm{avg}}=\frac{1}{\omega}\begin{bmatrix}0&1&0&0&0&0&0\\0&0&1&0&0&0&0\\-a_3&-a_2&-a_1&0&0&0&0\\0&0&0&0&1&0&0\\0&0&0&0&0&1&0\\0&0&0&-b_3&-b_2&-b_1&0\\0&0&0&0&0&0&-h\end{bmatrix}, \tag{31}$$

where $a_1=-p_x$, $a_2=\alpha c_x k_x q_x$, $a_3=-\alpha c_x k_x q_x(z_x+h)$, $b_1=-p_y$, $b_2=\alpha c_y k_y q_y$, $b_3=-\alpha c_y k_y q_y(z_y+h)$. Therefore the characteristic function of J_{avg} is

$$D(\lambda)=(\lambda+h)(\lambda^3+a_1\lambda^2+a_2\lambda+a_3)(\lambda^3+b_1\lambda^2+b_2\lambda+b_3).$$

Since the sufficient and necessary condition for a third order polynomial to have positive roots is $a_1, a_2, a_3>0$ and $a_1a_2-a_3>0$. Then, J_{avg} will be Hurwitz if and only if the following inequalities hold:

$$-p_x>0, \tag{32}$$
$$\alpha c_x k_x q_x>0, \tag{33}$$
$$-\alpha c_x k_x q_x(z_x+h)>0, \tag{34}$$
$$-\alpha c_x k_x p_x q_x+\alpha c_x k_x q_x(z_x+h)>0, \tag{35}$$
$$-p_y>0, \tag{36}$$
$$\alpha c_y k_y q_y>0, \tag{37}$$
$$-\alpha c_y k_y q_y(z_y x+h)>0, \tag{38}$$
$$-\alpha c_y k_y p_y q_y+\alpha c_y k_y q_y(z_y x+h)>0, \tag{39}$$
$$h>0. \tag{40}$$

One possible design to satisfy those inequalities (32)–(40) of the x loop is $\alpha, h, c_x, c_y, k_x, k_y, >0$ and $z_x, z_y<-h$, $p_x<z_x+h$, $p_y<z_y+h$.

Theorem 2. *Consider the system in Fig. 2, where the nonlinear map has the form of (2). There exists $\bar{\omega}$ such that for all $1/\omega\in(0,1/\bar{\omega})$ the system has a unique exponentially stable periodic solution $(\tilde{x}^{2\pi/\omega}, \tilde{y}^{2\pi/\omega}, e^{2\pi/\omega})$ of period $2\pi/\omega$ and this solution satisfies*

$$\left\|\begin{bmatrix}\tilde{x}^{2\pi/\omega}\\ \tilde{y}^{2\pi/\omega}\\ \tilde{v}_x^{\,2\pi/\omega}\\ \tilde{v}_y^{\,2\pi/\omega}\\ e^{2\pi/\omega}+\frac{\alpha^2}{2}(q_x+q_y)\\ w_x^{2\pi/\omega}\\ w_y^{2\pi/\omega}\end{bmatrix}\right\|\leqslant O(1/\omega),\quad \forall\tau\geqslant 0. \tag{41}$$

Hence $\lim\sup_{\tau\to\infty}|f-f^*|=O(\alpha^2+(1/\omega)^2)$.

Simulation results for a slowly time varying target (17)–(18) are shown in Fig. 6 for $a_m=1$, $\omega_m=0.1$, $\phi_m=3$, $f^*=1$, $q_x=1$, $q_y=0.5$, and $\omega=30$, $\alpha=0.05$, $c_x=c_y=20$, $h=1$. The parameters of the PD compensator are chosen to satisfy the inequalities (40), where $k_c=2$, $z_0=-2$, $p_0=-5$. The start position of the autonomous vehicle is $(x(0), y(0))=(1,1)$. As expected, tracking with a vehicle that has a double integrator in its input–output relation is harder than with a vehicle with a single integrator, but the use of a phase lead compensator helps achieve comparable performance.

4. A plant with moderately unstable poles

In this section we present an example of an MIMO plant with slightly unstable poles that can be stabilized, in the absence of its output measurements, with extremum seeking. This example is unrelated to the autonomous vehicle problem studied in the rest of the paper. Consider the two-input-two–output system

$$\dot{x}=\varepsilon_x x+v_x,\quad \dot{y}=\varepsilon_y y+v_y, \tag{42}$$

where $\varepsilon_x, \varepsilon_y>0$ are constant and v_x, v_y are the inputs. The ES scheme in Fig. 3 employs phase lead compensators for achieving robustness against the destabilizing effect of $\varepsilon_x, \varepsilon_y>0$.

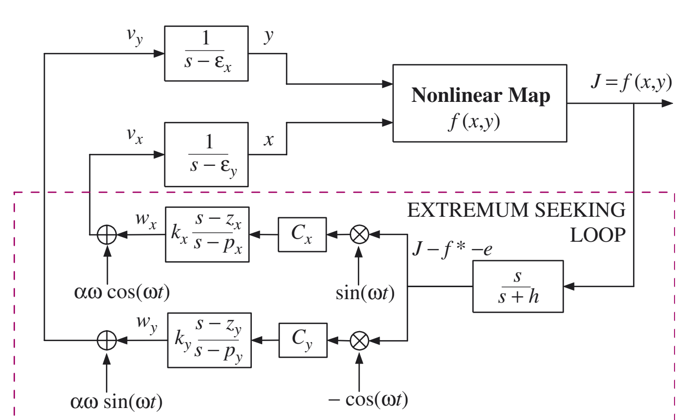

Fig. 3. Extremum seeking with unstable poles.

If $\varepsilon_x, \varepsilon_y$ are very small, the robustness of the extremum seeking loop itself will be able to compensate their effect without resorting to the phase lead. This simple extension of the single-integrator result is given without a proof.

Theorem 3. *Consider the system in Fig. 3 without the phase lead compensator, where the nonlinear map has the form of (2). There exist* $\bar{\varepsilon}, \bar{\omega}$ *such that for all* $\varepsilon_x, \varepsilon_y \in (0, \bar{\varepsilon})$ *and for all* $1/\omega \in (0, 1/\bar{\omega})$ *the system has a unique exponentially stable periodic solution* $(\tilde{x}^{2\pi/\omega}, \tilde{y}^{2\pi/\omega}, e^{2\pi/\omega})$ *of period* $2\pi/\omega$ *and this solution satisfies*

$$\left\| \begin{bmatrix} \tilde{x}^{2\pi/\omega} - \tilde{x}^e_{\text{avg}} \\ \tilde{y}^{2\pi/\omega} - \tilde{y}^e_{\text{avg}} \\ e^{2\pi/\omega} - e^e_{\text{avg}} \end{bmatrix} \right\| \leqslant O(1/\omega), \quad \forall \tau \geqslant 0, \tag{43}$$

where

$$\tilde{x}^e_{\text{avg}} = \frac{\varepsilon_x x^*}{\alpha c_x q_x - \varepsilon_x}, \quad \tilde{y}^e_{\text{avg}} = \frac{\varepsilon_y y^*}{\alpha c_y q_y - \varepsilon_y}$$

and

$$e^e_{\text{avg}} = -\left[\frac{\alpha^2}{2}(q_x + q_y) + q_x \left(\frac{\varepsilon_x x^*}{\alpha c_x q_x - \varepsilon_x} \right)^2 + q_y \left(\frac{\varepsilon_y y^*}{\alpha c_y q_y - \varepsilon_y} \right)^2 \right].$$

Moreover, $\limsup_{\tau \to \infty} |f - f^*| = O(\alpha^2 + (1/\omega)^2 + \varepsilon^2)$.

If, however, ε_x and ε_y in (42) are not very small but of medium size, then the robustness of the extremum seeking loop itself cannot stabilize the system, so we include a phase lead compensator to make up the phase lag introduced by the unstable first order dynamics. Then, in the time scale $\tau = \omega t$, we summarize the system in Fig. 3 as

$$\frac{\mathrm{d}\tilde{x}}{\mathrm{d}\tau} = \frac{1}{\omega}[w_x + \varepsilon_x(\tilde{x} + x^* + \alpha \sin\tau)], \tag{44}$$

$$\frac{\mathrm{d}\tilde{y}}{\mathrm{d}\tau} = \frac{1}{\omega}[w_y + \varepsilon_y(\tilde{y} + y^* - \alpha \cos\tau)], \tag{45}$$

$$\frac{\mathrm{d}e}{\mathrm{d}\tau} = \frac{h}{\omega}\Delta, \tag{46}$$

$$\frac{\mathrm{d}w_x}{\mathrm{d}\tau} = \frac{1}{\omega}\left[p_x w_x - c_x k_x z_x \Delta \sin\tau + c_x k_x \omega \Delta \cos(\omega t) + c_x k_x \frac{\mathrm{d}\Delta}{\mathrm{d}t} \sin(\omega t) \right], \tag{47}$$

$$\frac{\mathrm{d}w_y}{\mathrm{d}\tau} = \frac{1}{\omega}\left[p_y w_y + c_y k_y z_y \Delta \cos\tau + c_y k_y \omega \Delta \sin(\omega t) - c_y k_y \frac{\mathrm{d}\Delta}{\mathrm{d}t} \cos(\omega t) \right], \tag{48}$$

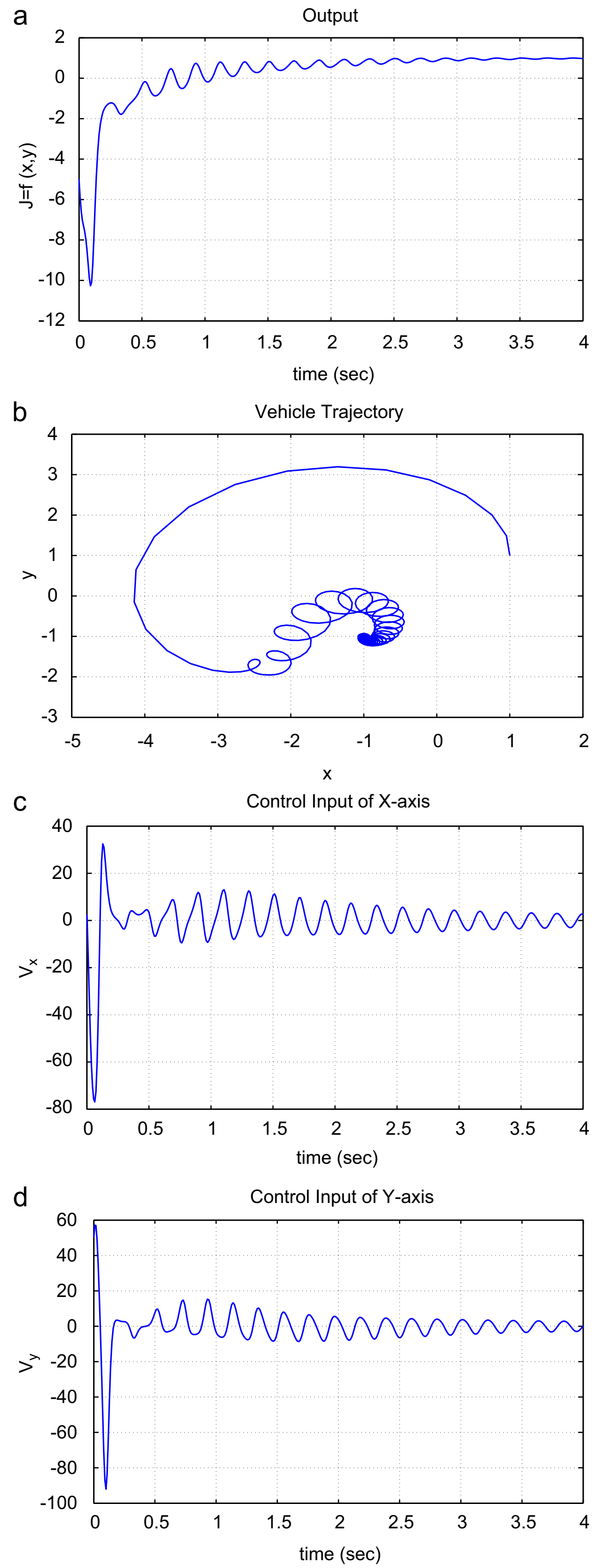

Fig. 4. Extremum seeking for velocity-actuated point mass, stationary case. (a) Output; (b) vehicle trajectory starts from (1,1); (c) control input of x-axis; (d) control input of y-axis.

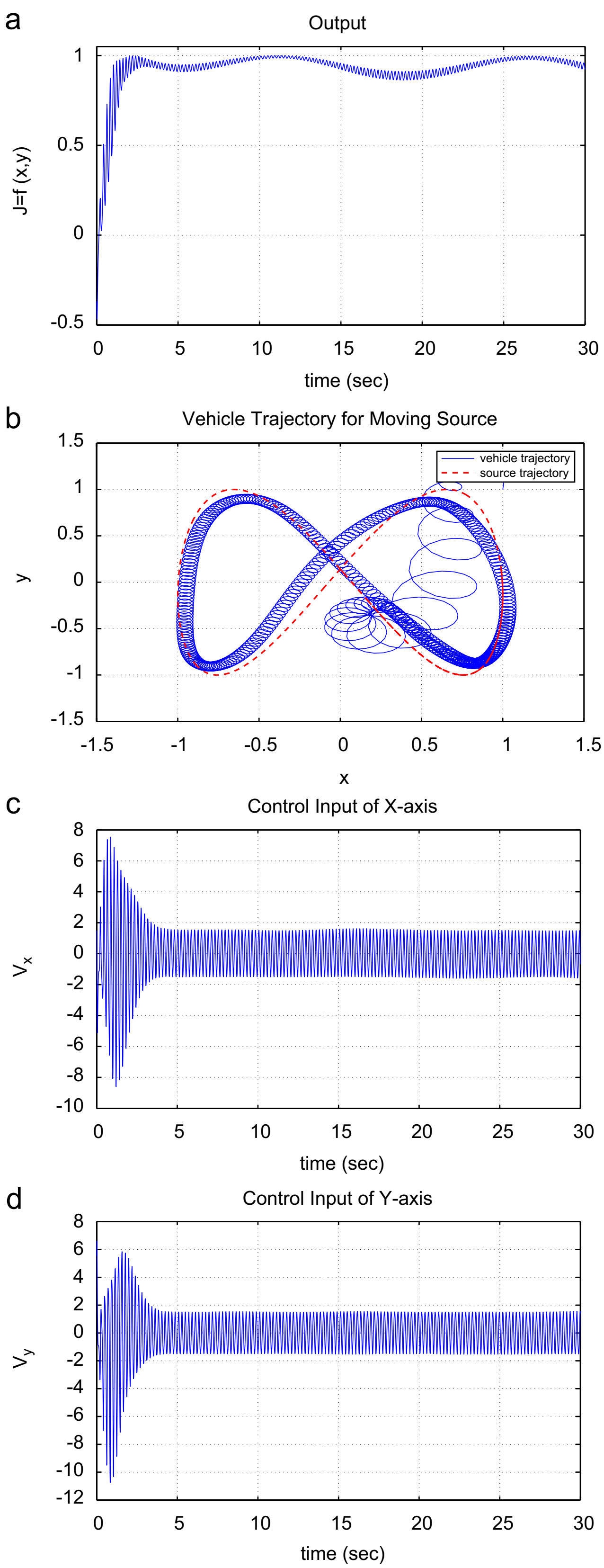

Fig. 5. Extremum seeking for velocity-actuated point mass, slowly time-varying case. (a) Output; (b) vehicle trajectory starts from (1,1) and source trajectory starts from (0,0); (c) control input of x-axis; (d) control input of y-axis.

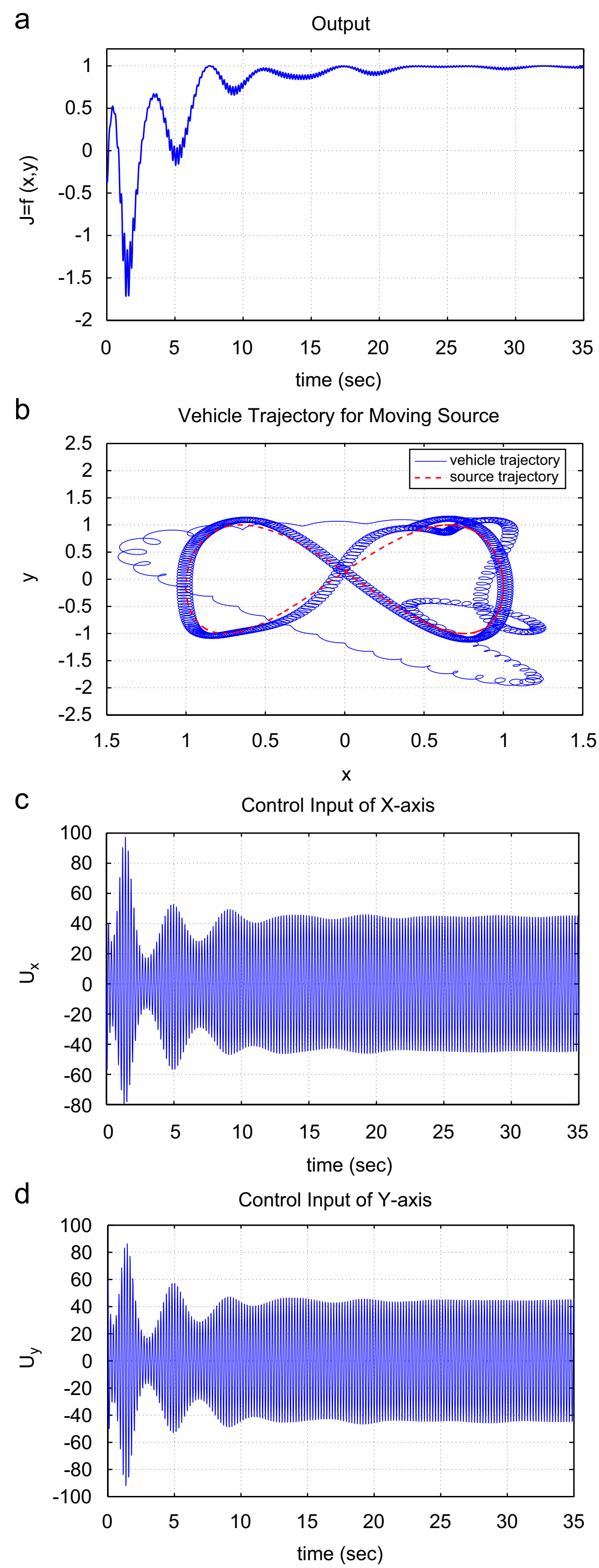

Fig. 6. Extremum seeking for force-actuated point mass, slowly time-varying case. (a) Output; (b) vehicle trajectory starts from (1,1) and source trajectory starts from (0,0); (c) control input of x-axis; (d) control input of y-axis.

where $\varDelta$ is defined in (6). The average model of (44)–(48) is

$$\frac{\mathrm{d}\tilde{x}_{\text{avg}}}{\mathrm{d}\tau} = \frac{1}{\omega}[\varepsilon_x(\tilde{x}_{\text{avg}} + x^*) + w_{x_{\text{avg}}}], \tag{49}$$

$$\frac{\mathrm{d}\tilde{y}_{\text{avg}}}{\mathrm{d}\tau} = \frac{1}{\omega}[\varepsilon_y(\tilde{y}_{\text{avg}} + y^*) + w_{y_{\text{avg}}}], \tag{50}$$

$$\frac{\mathrm{d}e_{\text{avg}}}{\mathrm{d}\tau} = \frac{1}{\omega}(-h)\left[q_x\tilde{x}^2_{\text{avg}} + q_y\tilde{y}^2_{\text{avg}} + e_{\text{avg}} + \frac{\alpha^2}{2}(q_x+q_y)\right], \tag{51}$$

$$\frac{\mathrm{d}w_{x_{\text{avg}}}}{\mathrm{d}\tau} = \frac{1}{\omega}[(p_x - \alpha c_x k_x q_x)w_{x_{\text{avg}}} + \alpha c_x k_x q_x(z_x - 2\varepsilon_x + h)\tilde{x}_{\text{avg}} - \alpha c_x k_x q_x \varepsilon_x x^*] \tag{52}$$

$$\frac{\mathrm{d}w_{y_{\text{avg}}}}{\mathrm{d}\tau} = \frac{1}{\omega}[(p_y - \alpha c_y k_y q_y)w_{y_{\text{avg}}} + \alpha c_y k_y q_y(z_y - 2\varepsilon_y + h)\tilde{y}_{\text{avg}} - \alpha c_y k_y q_y \varepsilon_y y^*]. \tag{53}$$

Then the equilibrium of the average model (49)–(53) is

$$\tilde{x}^e_{\text{avg}} = \frac{p_x\varepsilon_x x^*}{\alpha c_x k_x q_x(z_x - \varepsilon_x + h) - p_x\varepsilon_x}, \tag{54}$$

$$\tilde{y}^e_{\text{avg}} = \frac{p_y\varepsilon_y y^*}{\alpha c_y k_y q_y(z_y - \varepsilon_y + h) - p_y\varepsilon_y}, \tag{55}$$

$$e^e_{\text{avg}} = -\frac{\alpha^2}{2}(q_x+q_y) - q_x\left(\frac{p_x\varepsilon_x x^*}{\alpha c_x k_x q_x(z_x - \varepsilon_x + h) - p_x\varepsilon_x}\right)^2 - q_y\left(\frac{p_y\varepsilon_y y^*}{\alpha c_y k_y q_y(z_y - \varepsilon_y + h) - p_y\varepsilon_y}\right)^2, \tag{56}$$

$$w^e_{x_{\text{avg}}} = \frac{-\alpha c_x k_x q_x \varepsilon_x(z_x - \varepsilon_x + h)x^*}{\alpha c_x k_x q_x(z_x - \varepsilon_x + h) - p_x\varepsilon_x}, \tag{57}$$

$$w^e_{y_{\text{avg}}} = \frac{-\alpha c_y k_y q_y \varepsilon_y(z_y - \varepsilon_y + h)y^*}{\alpha c_y k_y q_y(z_y - \varepsilon_y + h) - p_y\varepsilon_y}. \tag{58}$$

The Jacobian of (53) at $(\tilde{x}^e_{\text{avg}}, w^e_{x_{\text{avg}}}, \tilde{y}^e_{\text{avg}}, w^e_{y_{\text{avg}}}, e^e_{\text{avg}})$ is

$$J_{\text{avg}} = \frac{1}{\omega}\begin{bmatrix} \varepsilon_x & 1 & 0 & 0 & 0 \\ a_1 & a_2 & 0 & 0 & 0 \\ 0 & 0 & \varepsilon_y & 1 & 0 \\ 0 & 0 & b_1 & b_2 & 0 \\ -2hq_x x^e_{\text{avg}} & 0 & -2hq_y y^e_{\text{avg}} & 0 & -h \end{bmatrix}, \tag{59}$$

where $a_1 = \alpha c_x k_x q_x(z_x - 2\varepsilon_x + h)$, $a_2 = (p_x - \alpha c_x k_x q_x)$, $b_1 = \alpha c_y k_y q_y(z_y - 2\varepsilon_y + h)$ and $b_2 = (p_y - \alpha c_y k_y q_y)$. Therefore, J_{avg} will be Hurwitz if and only if the following inequalities hold:

$$\alpha c_x k_x q_x - \varepsilon_x - p_x > 0, \tag{60}$$

$$(\alpha c_x k_x q_x + p_x)\varepsilon_x - \alpha c_x k_x q_x(z_x + h) > 0, \tag{61}$$

$$\alpha c_y k_y q_y - \varepsilon_y - p_y > 0, \tag{62}$$

$$(\alpha c_y k_y q_y + p_y)\varepsilon_y - \alpha c_y k_y q_y(z_y + h) > 0, \tag{63}$$

$$h > 0. \tag{64}$$

These conditions also ensure that the average equilibrium (54)–(58) is finite. If $q_x, q_y \geqslant \underline{q}$ and $\varepsilon_x, \varepsilon_y \leqslant \bar{\varepsilon}$, one possible design to satisfy the inequalities (60)–(64) is

(1) Choose $\alpha > 0$ to be small, $h > 0$.
(2) Choose $c_x > 0$, $k_x > 0$ such that $c_x k_x > \bar{\varepsilon}/2\alpha\underline{q}$.
(3) Choose $p_x = -\alpha c_x k_x \underline{q}$ and $z_x < -h$.

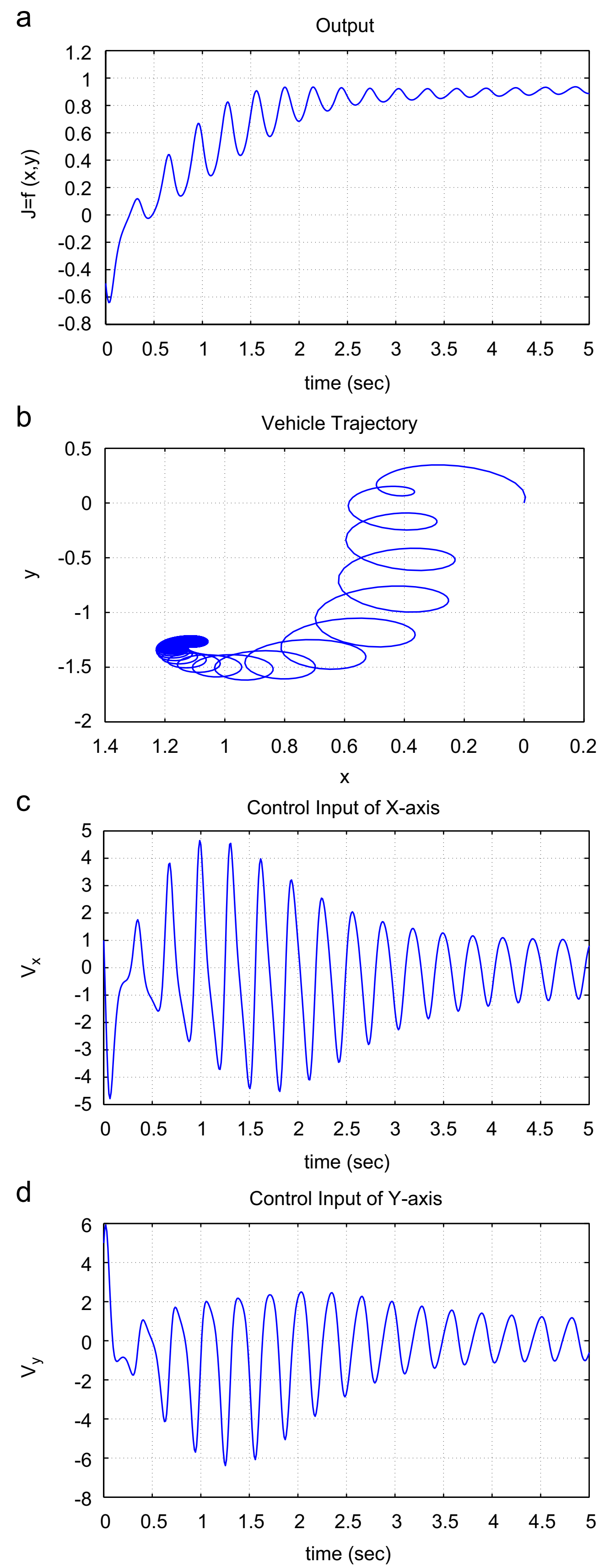

Fig. 7. Extremum seeking for unstable poles, stationary case. (a) Output; (b) vehicle trajectory starts from (0,0); (c) control input of x-axis; (d) control input of y-axis.

(4) Choose $c_y > 0$, $k_y > 0$ such that $c_y k_y > \bar{\varepsilon}/2\alpha \underline{q}$.
(5) Choose $p_y = -\alpha c_y k_y \underline{q}$ and $z_y < -h$.

Theorem 4. *Consider the system in Fig. 3, where the nonlinear map has the form of* (2). *If the conditions* (64) *are satisfied by design, then there exists* $\bar{\omega}$ *such that for all* $1/\omega \in (0, 1/\bar{\omega})$ *the system has a unique exponentially stable periodic solution* $(\tilde{x}^{2\pi/\omega}, \tilde{y}^{2\pi/\omega}, e^{2\pi/\omega})$ *of period* $2\pi/\omega$ *and this solution satisfies*

$$\left\| \begin{bmatrix} \tilde{x}^{2\pi/\omega} - \tilde{x}^e_{\mathrm{avg}} \\ \tilde{y}^{2\pi/\omega} - \tilde{y}^e_{\mathrm{avg}} \\ e^{2\pi/\omega} - e^e_{\mathrm{avg}} \\ w_x^{2\pi/\omega} - w^e_{x_{\mathrm{avg}}} \\ w_y^{2\pi/\omega} - w^e_{y_{\mathrm{avg}}} \end{bmatrix} \right\| \leqslant O(1/\omega), \quad \forall \tau \geqslant 0, \tag{65}$$

where $(\tilde{x}^e_{\mathrm{avg}}, \tilde{y}^e_{\mathrm{avg}}, e^e_{\mathrm{avg}}, w^e_{x_{\mathrm{avg}}}, w^e_{y_{\mathrm{avg}}})$ *is the equilibrium of the average model* (53).

Since

$$\begin{aligned} x - x^* &= \tilde{x} + \alpha \sin(\omega t) \\ &= (\tilde{x} - \tilde{x}^{2\pi/\omega}) \\ &\quad + \left(\tilde{x}^{2\pi/\omega} - \frac{p_x \varepsilon_x x^*}{\alpha c_x k_x q_x (z_x - \varepsilon_x + h) - p_x \varepsilon_x} \right) \\ &\quad + \frac{p_x \varepsilon_x x^*}{\alpha c_x k_x q_x (z_x - \varepsilon_x + h) - p_x \varepsilon_x} + \alpha \sin \tau, \end{aligned}$$

the theorem implies that the first term converges to zero, the second term is $O(1/\omega)$, the third term is $O(\bar{\varepsilon})$ and the fourth term $O(\alpha)$, guaranteeing $\lim\ \sup_{\tau\to\infty}|x-x^*|=O(\alpha+1/\omega+\bar{\varepsilon})$. Similarly, we can obtain $\lim\ \sup_{\tau\to\infty}|y-y^*|=O(\alpha+1/\omega+\bar{\varepsilon})$. Thus, eventually we get $\lim\ \sup_{\tau\to\infty}|f-f^*|=O(\alpha^2+(1/\omega)^2+\bar{\varepsilon}^2)$, so the residual error is proportional to the value of the unstable poles.

The robustness of the extremum seeking loop for slightly unstable poles is shown in Fig. 7 for $\varepsilon_x = \varepsilon_y = 0.05$, $\omega = 20$, $\alpha = 0.05$, $c_x = c_y = 10$, $h = 1$, $f^* = 1$, $q_x = 1$, $q_y = 0.5$, $(x(0), y(0)) = (0, 0)$. For considerably larger unstable poles, $\varepsilon_x = \varepsilon_y = 0.5$, a phase lead compensator is required and its use results in comparable performance as for $\varepsilon_x = \varepsilon_y = 0.05$ without a compensator.

The application of extremum seeking can be pursued in much greater generality than in the present section, allowing additional stable and fast dynamics, combined with unstable poles. This is a topic of future research.

Acknowledgments.

This research was supported by the National Science Foundation, Los Alamos National Laboratory, and a University of Dayton Graduate Student Summer Fellowship.

References

Ariyur, K. B., & Krstić, M. (2003). *Real-time optimization by extremum-seeking control*. Hoboken, NJ: Wiley-Interscience.

Banaszuk, A., Narayanan, S., & Zhang, Y. (2003). Adaptive control of flow separation in a planar diffuser. Paper AIAA-2003-0617. In *41st aerospace sciences meeting and exhibit*, Reno NV.

Khalil, H. K. (2001). *Nonlinear systems*. 3rd ed., Englewood Cliffs, NJ: Prentice-Hall.

Krstić, M., & Wang, H.-H. (2000). Design and stability analysis of extremum seeking feedback for general nonlinear systems. *Automatica*, *36*(2), 595–601.

Peterson, K., & Stefanopoulou, A. (2004). Extremum seeking control for soft landing of an electromechanical valve actuator. *Automatica*, *40*(6), 1063–1069.

Popovic, D., Jankovic, M., Manger, S., & Teel, A. R. (2003). Extremum seeking methods for optimization of variable cam timing engine operation. *Proceedings of the American control conference* (pp. 3136–3141). USA: Denver.

Li, Y., Rotea, M. A., Chiu, G. T.-C., Mongeau, L. G., & Paek, I.-S. (2005). Extremum seeking control of a tunable thermoacoustic cooler. *IEEE Transactions on Control Systems Technology*, *13*, 527–536.

Tan, Y., Nesic, D., & Mareels, I. (2005). On non-local stability properties of extremum seeking control. *Proceedings of the 16th IFAC world congress* Czeck Republic: Prague.

Zhang, C., Arnold, D., Ghods, N., Siranosian, A., & Krstic, M. (2007). Source seeking with nonholonomic unicycle without position measurement and with tuning of forward velocity. *Systems and Control Letters*, *56*, 245–252.

Zhang, X. T., Dawson, D. M., Dixon, W. E., & Xian, B. (2004). Extremum seeking nonlinear controllers for a human exercise machine. In *Proceedings of the IEEE conference on decision and control* Bahamas: Paradise Island.

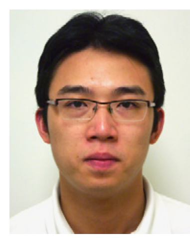

Chunlei Zhang received his B.S. degree from the Nanjing University of Science and Technology, Nanjing, China, in 1999, and the M.S. and Ph.D. degrees in Electrical Engineering from the University of Dayton in 2003 and 2006, respectively. He spent the Summer of 2005 as a visiting graduate student at the UC San Diego. He joined Etch Engineering Technology Control Group at Applied Materials in 2006 as a system design engineer. He is a member of the IEEE Robotics and Automation Society Technical Committee on Semiconductor Manufacturing Automation. His research interests include extremum seeking control and its applications, cooperative control of multiple autonomous agents and process control of semiconductor manufacturing equipment.

Antranik Siranosian received his B.S. degree in Mechanical Engineering from the Cal Ploy, Pomona in 2003. He received his M.S. in Dynamic Systems and Control from the UC San Diego in 2005, where he continues as a doctoral student. Antranik's research interests include nonlinear and adaptive control for shake tables and autonomous vehicles, as well as trajectory generation and tracking for finite and infinite dimensional systems.

Miroslav Krstic is the Sorenson Professor of Control Systems and Director of the Center for Control Systems and Dynamics at UC San Diego. He received his Ph.D. in 1994 from UC, Santa Barbara. He served as an Assistant Professor at the University of Maryland from 1995 until 1997. He is a coauthor of the books Nonlinear and Adaptive Control Design (1995), Stabilization of Nonlinear Uncertain Systems (1998), Flow Control by Feedback (2002), and Real-time Optimization by Extremum Seeking Control (2003). Krstic is the recipient of the NSF Career, ONR Young Investigator, and the PECASE awards. He has received the Axelby and Schuck best paper prizes, several student best paper awards, and the Best Dissertation Award at UCSD. He is a Fellow of IEEE and the first engineering professor to receive the UCSD Award for Excellence in Research (2005). He has served on the editorial boards of the IEEE Transactions on Automatic Control, Automatica, Systems and Control Letters, and International Journal of Adaptive Control and Signal Processing. He served as the Vice President for Technical Activities of the IEEE Control Systems Society and the Vice Chair of the Department of Mechanical and Aerospace Engineering at UCSD.